MULTI-SCALE ANALYSIS OF MECHANICAL PROPERTIES OF THREE-DIMENSIONAL BRAIDED CERAMIC MATRIX COMPOSITES WITH PORE DEFECTS

Xinyi Song [1], Shenghao Zhang [1], Di Zhang[1], Jin Zhou[1,*], Xuefeng Chen [1],
Zhongwei Guan [2] and W. J. Cantwell[3]
[1] School of Mechanical Engineering, Xi'an Jiao Tong University, Xi'an 710049, P. R. China
[2] Advanced Materials Research Centre, Technology Innovation Institute, Abu Dhabi, UAE
[3]Aerospace Engineering, Khalifa University, Abu Dhabi, UAE
[*] Corresponding author (jin.zhou@xjtu.edu.cn)

Keywords: 3D braided composite; Multiscale modeling; Damage mechanics; Pore defects

ABSTRACT

The multi-scale finite element model is developed to investigate the strength and damage behaviour of 3D braided composites with pore defects. The pore defects inside the composites are inspected and measured using CT scan. Based on the void data, the trans-scale numerical models are established, including the interface. Damage evolution under longitudinal tensile loading was evaluated. The effective properties are transferred from the fibre bundle scale to the mesoscale using the machine learning-based clustering method and further, the finite element model with pore defects is used to predict the macroscopic mechanical properties. Periodical boundary conditions are applied to the multi-scale FE models by the coupling and constraint equation, with defining commands available in Abaqus. It has been shown that the failure modes of yarn damage, matrix cracking and interface debonding are recognized and correspond well with the final failure morphology of the sample. The damage appears around the pore defects and then develops to the weak region in the matrix. Pore defects of the composites have a significant influence on the tensile behaviour of the composite, which is captured by the proposed multi-scale damage model. The porosity has a greater influence on the strength of the composite, in which the pore content increases by 10 % and the strength of the composite decreases 12 % approximatively. The validated models can be further used to predict the mechanical property of 3D braided composites with pore defects.

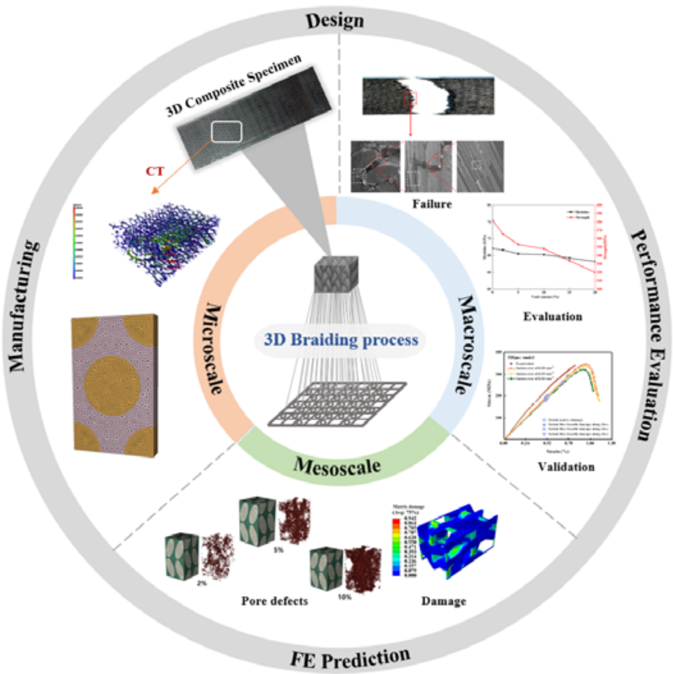

Graphic abstract

1 INTRODUCTION

Compared with two-dimensional (2D) laminated composites and two and half-dimensional (2.5D) woven composites, three-dimensional braided composites (3DBCs) present excellent performances in mechanical strength and stiffness, damage toleration and impact resistance [1–6]. The manufacturing process results in the high structural anisotropic and heterogeneous characteristics of this composite. It poses huge challenges for the accurate mechanical evaluation of 3D braided composites.

In recent decades, great efforts have been focused on analytical predictive models, such as fibre inclination model [7] and the three-cell model [8], which are widely used to evaluate the elastic properties of 3DBCs. Furthermore, Chen et al. [9], Zheng et al. [10] and Mahmood et al. [11] accounted the effect of the yarn cross-section shape on the elastic properties into their predictive models. However, the analytical models are not able to precisely predict the mechanical properties and failure modes due to the over-simplified assumptions [12]. It is crucial to determine the yarn architecture and void characteristics. X-ray computed tomography (CT), especially suitable for 3D nature characterization, can capture the failure process under loading [13,14], creates cross-sectional images of the object and differentiates materials by the degree of X-ray attenuation [15,16]. This non-destructive inspection technique has been used to the 3D assessment of braided composites. Fang and Liu [17,18] reconstructed the topology geometry of 3D four-directional and five-directional braided composites for elastic analyses. Melenka et al. [19,20] identified the porosity and strand geometry of 2D tubular braided composites and bio-based braided composite structures by high-resolution CT. Ya et al. [21] characterized the yarn and porosity from the reconstructed 3D model by Micro-CT. The above-mentioned studies have only discussed scanning results in one scale with limited resolution, and none has conducted multi-scale strength and damage analyses of 3D braided composites based on CT data.

In this study the multi-scale finite element model is developed to investigate the strength and damage behaviour of 3D braided composites with pore defects. The pore defects inside the composites are inspected and measured using CT scan. Based on the void data, the trans-scale numerical models are established with interfaces. Damage evolution under longitudinal tensile loading is evaluated. The present scheme provides a tool for accurately performing the mechanical analyses of braided composites with pore defects based on the real geometric information.

2. EXPERIMENTAL DETAILS

The tensile and compressive tests were conducted on a DNS200 electromechanical testing machine with a displacement control of 1 mm/min, following the ASTM D3039 [22] standards. Strain gauges were attached to specimens to record their strain response, as shown in Figure 1. Each test was repeated 5 times, and the related average value was used as the final result to ensure accuracy.

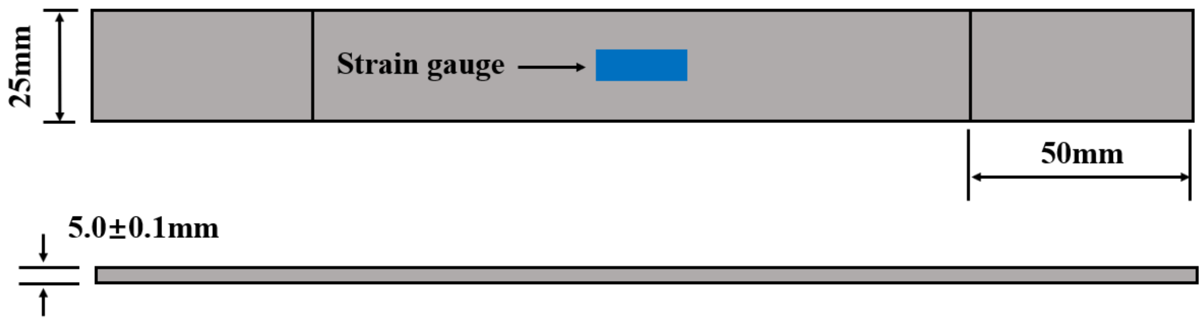

Figure 1: Size of specimen.

A Xradia 610 Versa microscope with a 20 × lens detector, is performed to scan samples of 3DBCs. A fundamental assumption of the proposed methodology is that the scanned samples are representative of the same batch of braided composites. To get enough spatial resolution, the sample is cut to the size of 4 mm × 4 mm × 5 mm. After scanning, the yarns and pore defects are reconstructed by AVIZO 9.0 software package. The void contents are calculated to be about 5 %.

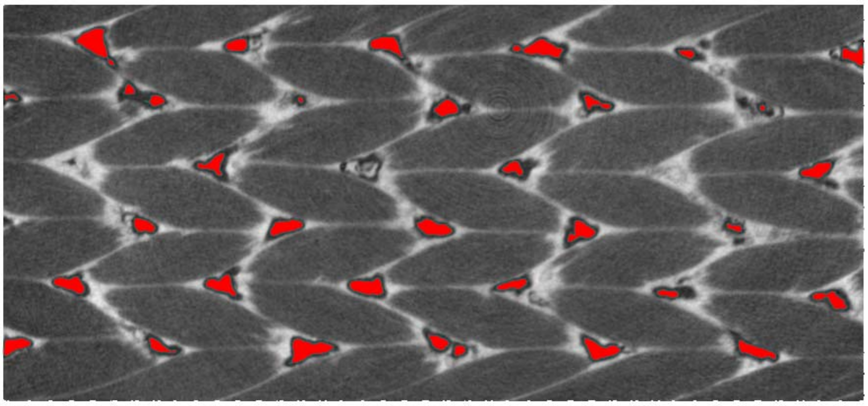

Figure 2: CT scanning results of 3d braided ceramic matrix composites.

3. CT BASED MULTI-SCALE NUMERICAL MODEL

3.1. Micro-scale RVC model with voids for yarns

For micro RVEs, fibers with radius of 3.5 μm are constructed. Also, the pore defects with the size and content obtained by CT data are randomly constructed by a Python script. To keep the structural periodicity of RVEs under deformation, the corresponding mesh nodes are produced on parallel faces to impose periodical boundary conditions (PBCs). The tetrahedron elements (C3D4) are used to mesh the micro RVEs, as shown in Fig. 3.

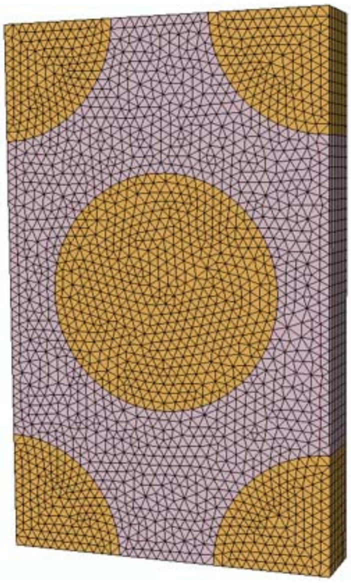

Figure 3: RVE model of yarns

3.2 Meso-scale RVC model with voids for braided composites

According to the CT data, the interior braiding angle of 39.5°and width of 2.4 mm are applied to construct the meso RVC with a parametric modeling method which is created by SolidWorks. The configuration of yarns in the meso RVE is depicted in Fig. 4. The tetrahedron elements (C3D4) are meshed in the meso RVEs. The elements of matrix are randomly chosen and then the properties are reduced by 99.99% to simulate the voids. Totally, the void content constituted by the established large and small pore defects is about 5%, which is determined by CT characterization. In addition, in order to predict the effect of pore content on mechanical properties, the finite element models with porosity of 2% and 10% were established.

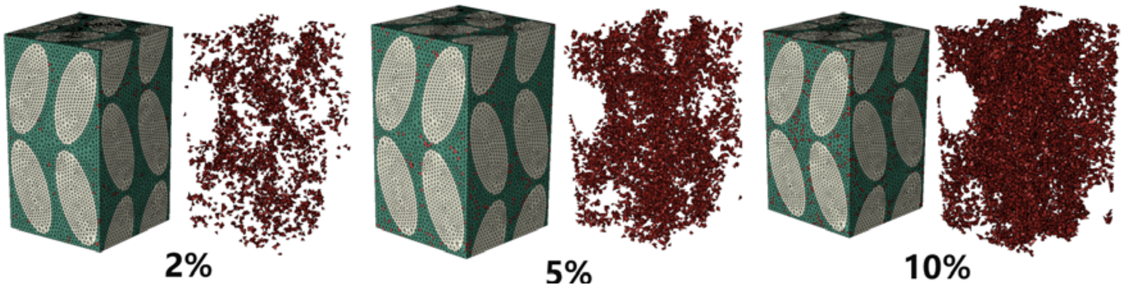

Figure 4: The finite element models with different porosity.

3.3 The progressive damage model

The spatial compositions of a 3D braided composite is extremely complex, which are the associated failure modes. The fiber and matrix can be analyzed using different failure criteria. The fiber bundle can be considered as a transversely isotropic material, whereas the matrix is assumed to be isotropic. The 3D Hashin criteria have been successfully used to predict longitudinal tensile damage in fiber reinforced composite materials, these criteria are described as follows:

$$F_{\mathrm{xt}}{}^{2}=\left(\frac{\sigma_{xx}}{T_{\mathrm{x}}}\right)^{2}+\frac{\sigma_{xy}{}^{2}}{S_{\mathrm{xy}}{}^{2}}+\frac{\sigma_{xz}{}^{2}}{S_{xz}{}^{2}}\geq 1,\quad (\sigma_{xx}\geq 0) \tag{1}$$

$$F_{\mathrm{xc}}{}^{2}=\left(\frac{\sigma_{xx}}{C_{\mathrm{x}}}\right)^{2}+\frac{\sigma_{xy}{}^{2}}{S_{xy}{}^{2}}+\frac{\sigma_{xz}{}^{2}}{S_{xz}{}^{2}}\geq 1,\quad (\sigma_{xx}< 0) \tag{2}$$

$$F_{\mathrm{yt}}{}^{2}=\left(\frac{\sigma_{yy}}{T_{y}}\right)^{2}+\frac{\sigma_{xy}{}^{2}}{S_{xy}{}^{2}}+\frac{\sigma_{yz}{}^{2}}{S_{yz}{}^{2}}\geq 1,\quad (\sigma_{yy}\geq 0) \tag{3}$$

$$F_{\mathrm{yc}}{}^{2}=\left(\frac{\sigma_{yy}}{C_{y}}\right)^{2}+\frac{\sigma_{xy}{}^{2}}{S_{xy}{}^{2}}+\frac{\sigma_{yz}{}^{2}}{S_{yz}{}^{2}}\geq 1,\quad (\sigma_{yy}< 0) \tag{4}$$

$$F_{\mathrm{zt}}{}^{2}=\left(\frac{\sigma_{zz}}{T_{z}}\right)^{2}+\frac{\sigma_{xz}{}^{2}}{S_{xz}{}^{2}}+\frac{\sigma_{yz}{}^{2}}{S_{yz}{}^{2}}\geq 1,\quad (\sigma_{zz}\geq 0) \tag{5}$$

$$F_{\mathrm{zc}}{}^{2}=\left(\frac{\sigma_{zz}}{C_{z}}\right)^{2}+\frac{\sigma_{xz}{}^{2}}{S_{xz}{}^{2}}+\frac{\sigma_{yz}{}^{2}}{S_{yz}{}^{2}}\geq 1,\quad (\sigma_{zz}< 0) \tag{6}$$

where T is the tensile strength, C is the compression strength and S is the material shear strengths.

The damage criterion proposed by Christensen is adopted herein to study matrix damage, which can be used to accurately capture the damage and yield characteristics of an isotropic material subjected to a range of stress states.

$$F_{\mathrm{m}}{}^{2}=\left(\frac{1}{T_{\mathrm{m}}}-\frac{1}{C_{\mathrm{m}}}\right)(\sigma_{xx}+\sigma_{yy}+\sigma_{zz})+\frac{1}{T_{\mathrm{m}}C_{\mathrm{m}}}\left\{\frac{1}{2}[(\sigma_{xx}-\sigma_{yy})^{2}+(\sigma_{yy}-\sigma_{zz})^{2}+(\sigma_{zz}-\sigma_{xx})^{2}]+3(\sigma_{xy}{}^{2}+\sigma_{xz}{}^{2}+\sigma_{yz}{}^{2})\right\}\geq 1 \tag{7}$$

The user-defined subroutines UMATs are implemented in ABAQUS/STANDARD to simulate the failure behavior of yarns and braided composites.

3 RESULTS AND DISCUSSION

3.1 Effect of pore defects on mechanical behavior

The simulation results of 5 % pore content agree well with the experimental results. The finite element simulation of different pore gradients shows that the modulus and strength of composites decrease with the increase of pore content. The porosity has a great influence on the strength of composite materials. Therefore, reducing the porosity content in the manufacturing process has a significant influence on improving the mechanical properties of composite materials.

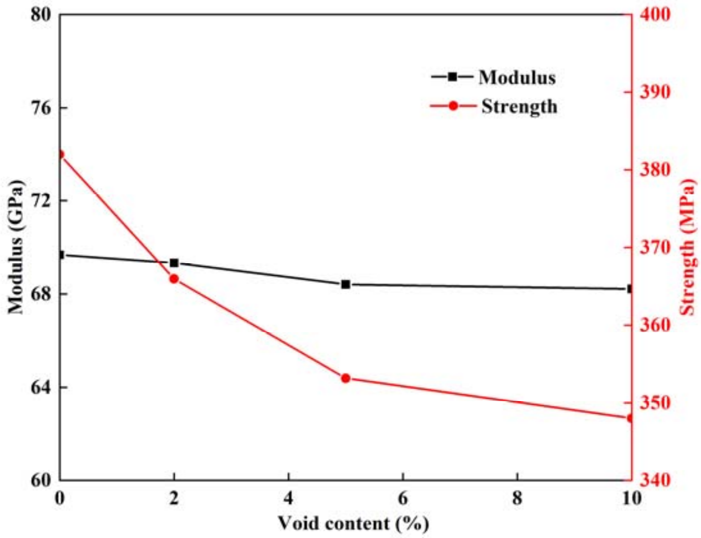

Figure 5: Influences of void content on the modulus and strength

3.2 Damage mechanisms analysis

The tensile fracture morphology of 3D braided C/SiC composites is observed by SEM. The tensile strength of SiC matrix is much smaller compared with the fiber, so that the matrix cracks first and the cracking originated from the pores and microcracks in the preparation process (Fig. 6a). When the matrix cracking is saturated, the load begins to transfer to the fiber. Therefore, the fiber produces longitudinal tensile deformation, and the inclined braiding fiber is subjected to the extrusion from the matrix and shear force during rotation. After reaching the maximum stress value, braiding fibers shear fracture occurs. With the strong bonding force between the fibers and the matrix, the microcracks converge at the interface without deflection and penetrate directly through the fibers, and the braiding fibers are pulled out, as shown in (Fig. 6b). Finally, corresponding the stress–strain curve of 3D braided C/SiC composites, the experimental curve drops rapidly when the maximum stress is reached and shows obvious brittle fracture characteristics. Overall, the damage process of 3D braided composites under longitudinal static tension is more complex. The damage modes mainly include shear fracture of the braiding yarn and matrix cracking.

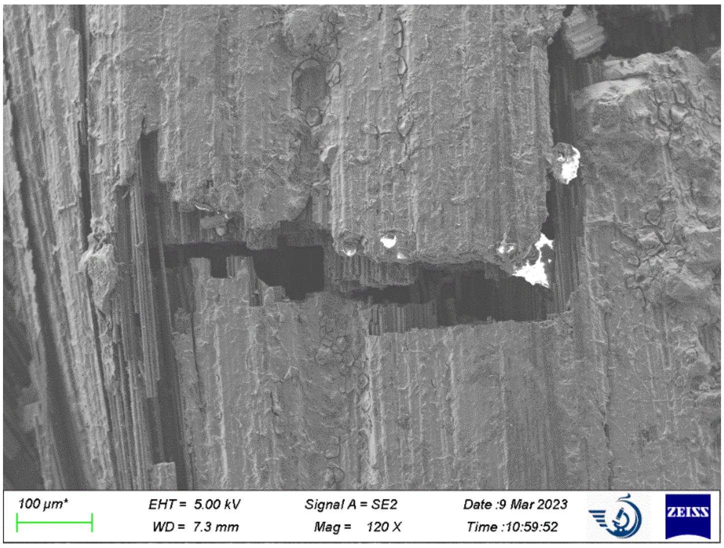

(a)

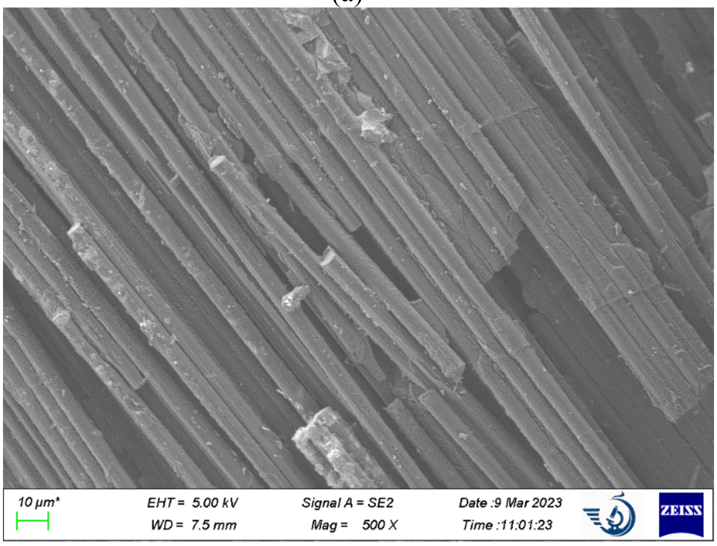

(b)

Figure 6: Tensile fracture morphology

4 CONCLUSIONS

In this paper, a multiscale modeling method is proposed and established to predict the elastic behavior of 3DBCs composites with pore defects. The parametric effects of void characteristics and braiding features have been conducted for yarns and 3D braided composites. Based on the study, the following conclusions have been drawn. As for braided composites, the modelling results by the multi-scale method with pore defects show good agreement with the corresponding experimental data. This indicates that the present multiscale analysis scheme is effective in predicting the elastic behavior of 3DBCs.

REFERENCES

[1] M. T arfaoui, M. Nachtane. Can a three-dimensional composite really provide better mechanical performance compared to two-dimensional composite under compressive loading?, *Journal of Reinforced Plastics and Composites*, **38**(2) , 2019, pp.49-61(doi: doi.org/10.1177/0731684418802028).

[2] H. Zuo, D. Li, L. Jiang. High temperature mechanical response and failure analysis of 3D five-directional braided composites with different braiding angles, *Materials*, **12**(21), 2019, P.3506(doi: doi.org/10.3390/ma12213506).

[3] L. Wu, W. Wang, Q. Jiang, et al. Mechanical characterization and impact damage assessment of hybrid three-dimensional five-directional composites, *Polymers*, **11**(9), 2019, p.1395(doi: doi.org/10.3390/polym11091395).
[4] F. Ahmad, N. Yuvaraj, P.K. Bajpai. Effect of reinforcement architecture on the macroscopic mechanical properties of fiberous polymer composites: A review, *Polymer Composites*, **41**(6) , 2020, pp.2518-2534 (doi: doi.org/10.1002/pc.25666).
[5] A.N. Dickson, D.P. Dowling. Enhancing the bearing strength of woven carbon fibre thermoplastic composites through additive manufacturing, *Composite Structures*, **212**, 2019, pp.381-388(doi: doi.org/10.1016/j.compstruct.2019.01.050).
[6] Y. Li, X. Chen, J. Zhou, et al. A review of high-velocity impact on fiber-reinforced textile composites: Potential for aero engine applications, *International Journal of Mechanical System Dynamics*, **2**(1), 2022, pp.50-64(doi: doi.org/10.1002/msd2.12033).
[7] J.M. Yang, C.L. Ma, T.W. Chou. Fiber inclination model of three-dimensional textile structural composites, *Journal of composite Materials*, **20**(5) ,1986, pp.472-484(doi: doi.org/10.1177/002199838602000050).
[8] D.L. Wu. Three-cell model and 5D braided structural composites, *Composites Science and Technology*, **56**(3), 1996, pp.225-233(doi: doi.org/10.1016/0266-3538(95)00136-0).
[9] C. Li, X.M. Tao, C.L. Choy. On the microstructure of three-dimensional braided performs, *Composites Science and technology*, **59**(3), 1999, pp.391-404(doi: doi.org/10.1016/S0266-3538(98)00079-7).
[10] X.T. Zheng, T. YE. Microstructure analysis of 4-step three-dimensional braided composite, *Chinese Journal of Aeronautics*, **16**(3), 2003, pp.142-150(doi: doi.org/10.1016/S1000-9361(11)60175-1).
[11] M.M. Shokrieh, M.S. Mazloomi. A new analytical model for calculation of stiffness of three-dimensional four-directional braided composites, *Composite Structures*, **94**(3), 2012, pp.1005-1015(doi: doi.org/10.1016/j.compstruct.2011.09.010).
[12] A. Hallal, R. Younes, F. Fardoun. Review and comparative study of analytical modeling for the elastic properties of textile composites, *Composites Part B: Engineering*, **50**, 2013, pp.22-31(doi: doi.org/10.1016/j.compositesb.2013.01.024).
[13] Y. Chai, Y. Wang, Z. Yousaf, et al. Following the effect of braid architecture on performance and damage of carbon fibre/epoxy composite tubes during torsional straining, *Composites Science and Technology*, **200**, 2020, p.108451(doi: doi.org/10.1016/j.compscitech.2020.108451).
[14] Y. Chai, Y. Wang, Z. Yousaf, et al. Damage evolution in braided composite tubes under torsion studied by in-situ X-ray computed tomography, *Composites Science and Technology*, **188**, 2020, p.107976(doi: doi.org/10.1016/j.compscitech.2019.107976).
[15] S.C. Garcea, Y. Wang, P.J. Withers. X-ray computed tomography of polymer composites, *Composites Science and Technology*, **156**, 2018, pp.305-319(doi: doi.org/10.1016/j.compscitech.2017.10.023).
[16] K. Naresh, K.A. Khan, R. Umer, et al. The use of X-ray computed tomography for design and process modeling of aerospace composites: A review, *Materials & Design*, **190**, 2020, p.108553(doi: doi.org/10.1016/j.matdes.2020.108553).
[17] G. Fang, C. Chen, S. Yuan, et al. Micro-tomography based geometry modeling of three-dimensional braided composites, *Applied Composite Materials*, **25**, 2018, pp.469-483(doi: 10.1007/s10443-017-9630-8).
[18] X. Liu, D. Zhang, J. Sun, et al. Refine reconstruction and verification of meso-scale modeling of three-dimensional five-directional braided composites from X-ray computed tomography data, *Composite Structures*, **245**, 2020, p.112347(doi: doi.org/10.1016/j.compstruct.2020.112347).
[19] G.W. Melenka, E. Lepp, B.K.O. Cheung, et al. Micro-computed tomography analysis of tubular braided composites, *Composite Structures*, **131**, 2015, pp.384-396(doi: doi.org/10.1016/j.compstruct.2015.05.057).
[20] G.W. Melenka, B.M. Bruni-Bossio, C. Ayranci, et al. Examination of voids and geometry of bio-based braided composite structures, *IOP Conference Series: Materials Science and Engineering. IOP Publishing*, **406**(1), 2018, p.012012(doi: 10.1088/1757-899X/406/1/012012).

[21] J. Ya, Z. Liu, Y. Wang. Micro-CT characterization on the meso-structure of three-dimensional full five-directional braided composite, *Applied Composite Materials*, **24**, 2017, p.593-610(doi: 10.1007/s10443-016-9528-x).
[22] Standard A. Standard test method for tensile properties of polymer matrix composite materials[J]. ASTM D3039/DM, **3039**, 2008.